

# CYBER AIDD

## WEEKLY REPORT



**Cyber-AIDD analysis of the of PARK7 Target molecules**

(Reference from: *Journal of Medicinal Chemistry*, 2024, 67,10,7935-7953)

# Cyber-AIDD Analysis of PARK7/DJ-1 Inhibitors, probes and PROTACs Discovery and optimization

## Part 1

The integration of multiple chemical tools such as small molecule inhibitors, activity-based probes (ABPs), and proteolysis targeting chimeras (PROTACs) has advanced clinical drug discovery and facilitated the exploration of various biological aspects of targeted proteins. This article reports Chemical tools developed against human Parkinson's disease protein 7 (PARK7/DJ-1), which is associated with Parkinson's disease and cancer, were developed. By combining structure-guided design, miniaturized library synthesis, and high-throughput screening, two potent compounds, JYQ-164 and JYQ-173, were identified to inhibit PARK7 in vitro and in cells by covalently and selectively targeting its key residue Cys106. Using JYQ-173, a cell-permeable Bodipy probe, JYQ-196, was further developed for covalent labeling of PARK7 in living cells, as well as a first-in-class PARK7 degrader, JYQ-194, which selectively induces its proteasomal degradation in cells. The study provides valuable Chemical Tools to enhance understanding of PARK7 biology in the cellular context and provide opportunities for therapeutic intervention supply A new opportunity.

Pharmacodia CyberSAR system provides in-depth analysis of PARK7 target molecules. The system displays active molecules related to the target through **clustered structure views** and **original structure views**, and presents potential hits in the form of a timeline during the R&D stage. In addition, CyberSAR also provides visual analysis of **indications** and experimental designs to help R&D personnel quickly obtain target structure information and open up research ideas. Although CyberSAR has not been used in the initial development of molecules, it shows great application potential in analyzing and optimizing drug molecules.

Journal of Medicinal Chemistry > Vol 67/Issue 10 > Article

Open Access

ARTICLE | May 7, 2024

### Development of Inhibitors, Probes, and PROTAC Provides a Complete Toolbox to Study PARK7 in the Living Cell

Yujing Jia, Merve Oyken, Robbert Q. Kim, Rayman T.N. Tjokrodjirjo, Arnoud H. de Ru, Antonius P. A. Janssen, Stephan M. Hacker, Peter A. van Veele, Paul P. Geurink\*, and Aysegül Sağmaz\*

Cite Share Jump to Expand



Journal of Medicinal Chemistry

Cite this: *J. Med. Chem.* 2024, 67, 10, 7935–7953

<https://doi.org/10.1021/acs.jmedchem.3c02410>

Published May 7, 2024

Copyright © 2024 The Authors. Published by American Chemical Society. This publication is licensed under [CC-BY 4.0](https://creativecommons.org/licenses/by/4.0/)

## Part 2

Human Parkinson's disease protein 7 (PARK7), also known as DJ-1, is a small (~20kDa) multifunctional protein associated with various types of cancer and Parkinson's disease. Over the years, PARK7 has been found to play a role in protecting cells from stress conditions, especially oxidative stress. The key element of PARK7 function is the highly conserved cysteine residue at position 106. Cys106 is the active site residue for the enzymatic glyoxalase activity of PARK7, and the oxidation of Cys106 is essential for PARK7 to achieve non-enzymatic functions, including antioxidant, molecular chaperone, co-transcription factor and anti-apoptotic/ferroptosis functions. On the other hand,,Excessive oxidation of the Cys106 residue leads to the loss of its neuroprotective activity and the development of neurodegenerative diseases.

Its key roles in multiple biological processes, including cytoprotective/survival activities and promotion of tumorigenesis, make PARK7 an attractive therapeutic target. However, how exactly PARK7 achieves its multiple functions remains to be explored. This highlights the need for potent inhibitors and degraders that specifically target PARK7 in cells to explore PARK7 biology and advance drug discovery. Initially, some small molecule inhibitors were identified that bind to PARK7. This was later expanded by a group of inhibitors based on the endogenous metabolite isatin, which binds PARK7 and reacts covalently with Cys106. Aminoepoxycyclohexanones have also been reported to covalently modify Cys106, and the inclusion of an alkyne moiety in these compounds allowed in situ analysis of PARK7 via a two-step labeling approach. We recently reported the development of a cyanamide-containing inhibitor, JYQ-88, as well as two fluorescent probe variants that covalently react with PARK7 Cys106 and demonstrated successful application of these compounds in cell lysates. However, to date, only a few compounds have been developed to bind to PARK7 in living cells. Development of the cell-permeable small molecule compound specifically targets the Cys106 residue of PARK7.

Starting from JYQ-88, a strategy combining structure-guided design, miniaturized synthesis and high-throughput screening was used to obtain the first-class PARK7 inhibitors JYQ-164 and JYQ-173. According to the simplified cysteine-based protein analysis of acid activity (SLC-ABPP) experiments have shown that both compounds specifically bind to PARK7 and in cells Cys106 reactions occur, in which JYQ-173 is the most effective one. In addition, use of Bodipy cell-permeable fluorescent probes JYQ-196. The results showed that covalent labeling of HEK293T and A549 cells with PARK7. Finally, it was also reported that PARK7 degraders JYQ-194, which induces PARK7. In summary, a complete PARK7 chemical toolbox to facilitate further research on their diverse functions and future drug development.

### **Combining structure-guided design and high-throughput synthesis to discover PARK7 inhibitors**

The recently reported PARK7 inhibitor JYQ-88 (Figure 1A) effectively inhibited PARK7 in cell lysates.

However, the compound was found to have poor cell permeability after administration to intact HEK293T cells. Therefore, optimization was performed using JYQ-88 as a starting point to further improve the inhibitory potency, specificity, and cellular uptake of this molecule. The crystal structure of the PARK7-JYQ-88 complex (PDB 7PA3) showed that the azidoacetyl moiety of JYQ-88 did not interact with PARK7, and the main hydrophilic pocket around this moiety was largely unoccupied (Figure 1B). Therefore, it was chosen to optimize the inhibitor by introducing different substituents to replace the azidomethyl moiety using two strategies. First, a small custom library was designed and synthesized to investigate whether the introduction of larger hydrophilic substituents on JYQ-88 would enhance the interaction with the PARK7 pocket. Five different hydrophilic moieties were introduced, including

morpholine, 4-methylpiperazine, 3-hydroxyphenyl, piperazine, and piperidine to replace the azidomethyl moiety (Figure 1C, compounds 1–5 in Scheme 1). The second approach involved a library of compounds with different substituents introduced at the azidomethyl position. This crude compound library was subjected to high-throughput screening using an in-house developed PARK7 fluorescence polarization (FP) assay. Compounds at a final concentration of 1  $\mu\text{M}$  were incubated with recombinant PARK7, followed by incubation with carboxyrhodamine-labeled JYQ-107, a reagent that labels any remaining active PARK7, and the FP signal was monitored. Overall, most compounds showed more than 50% inhibition, and 54 hit compounds that showed more than 90% inhibition were specifically selected (Figure 1E). All of these hit compounds could be validated at 1, 0.5, and 0.25  $\mu\text{M}$  concentrations in the same FP assay (Figure 1F, Supplementary Data S1). Since all compounds were present as a mixture in the library plate, the top 10 hit compounds were selected for resynthesis for biochemical characterization (Figure 1G, Scheme 1, Supplementary Data S1). Notably, the cyanamide precursors of all compounds (Figure 1D, left) also inhibited PARK7. In HTS, the crude mixture was found to have approximately 40% inhibition at 1  $\mu\text{M}$  (Figure 1E), but the inhibitory potency of the pure compound was 2.3% at 0.25  $\mu\text{M}$  and 2.5% at 0.5  $\mu\text{M}$ , respectively. Significant Reduced to 3% and 20%.

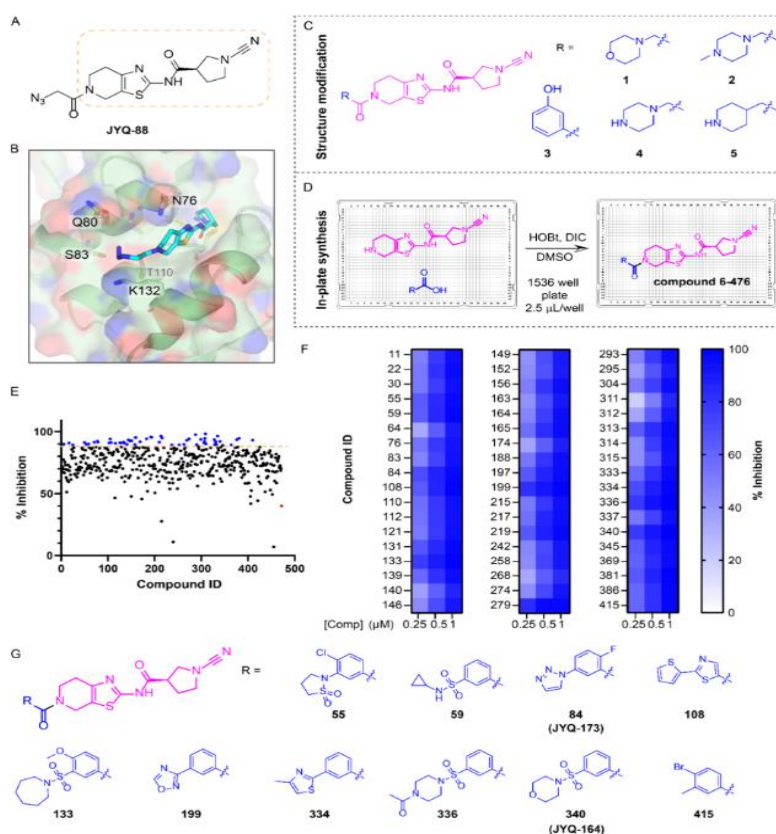


**Figure 1.** Discovery of improved PARK7 inhibitors. (A) Structure of PARK7 inhibitor JYQ-88. (B) Crystal structure of PARK7-JYQ-88 complex (PDB 7PA3) showing an unoccupied pocket around the azidoacetyl moiety. (C) Chemical structures of designed compounds with a hydrophilic substituent. (D) Schematic illustration of in-plate synthesis to build a compound library. (E) Screening results using an FP assay at 1  $\mu\text{M}$  compound concentration. Blue color represents compounds showing over 90% inhibition. Red color shows inhibition data for the amine precursor compound. (F) Heatmap displaying validation of the screening hits at 0.25, 0.5, and 1  $\mu\text{M}$  using the FP assay. (G) Chemical structures of the resynthesized top 10 compounds.

## JYQ-164 and JYQ-173 bind effectively to PARK7 in cells

Using FP experiment Fifteen pure compounds from two different approaches (5 compounds from structural modification and 10 compounds from HTS) were evaluated for their potency in inhibiting PARK7 at 0.25 and 1  $\mu$ M final concentrations (Figure 2A). 11 compounds showed better. Among them, compounds 84, 336, and 340 discovered by HTS showed the highest potency at 0.25  $\mu$ M, close to 100% inhibition, while compound 3 was the only compound derived from designed structural modification, only effectiveness slightly improved. With JYQ-88 in contrast, compounds with polar groups (Such as 4-methylpiperazine, piperazine and piperidine) decreased efficacy.

Since JYQ-88 is a potent in vitro inhibitor but did not show inhibition of intracellular PARK7 (Supporting Information Fig. S1), the cellular target effects of all 15 compounds were evaluated in a cell-based competition assay. HEK293T cells were treated with 5  $\mu$ M of the compounds for 24 h, followed by cell lysis and incubation of samples with the previously developed SulfoCy5 PARK7 probe JYQ-92, SDS-PAGE and analysis by fluorescence scanning and western blotting (Fig. 2B). Target binding of cellular PARK7 was reflected by the disappearance of the PARK7 labeled PARK7 in the fluorescence gel scan and the disappearance of the shifted probe labeled PARK7 in the western blot. This indicates that all 11 of the above potency-enhanced compounds were able to bind to PARK7 in cells, indicating improved cellular target binding. Notably, the remaining 4 compounds with reduced potency (1, 2, 4, 5) did not bind to PARK7 in cells.

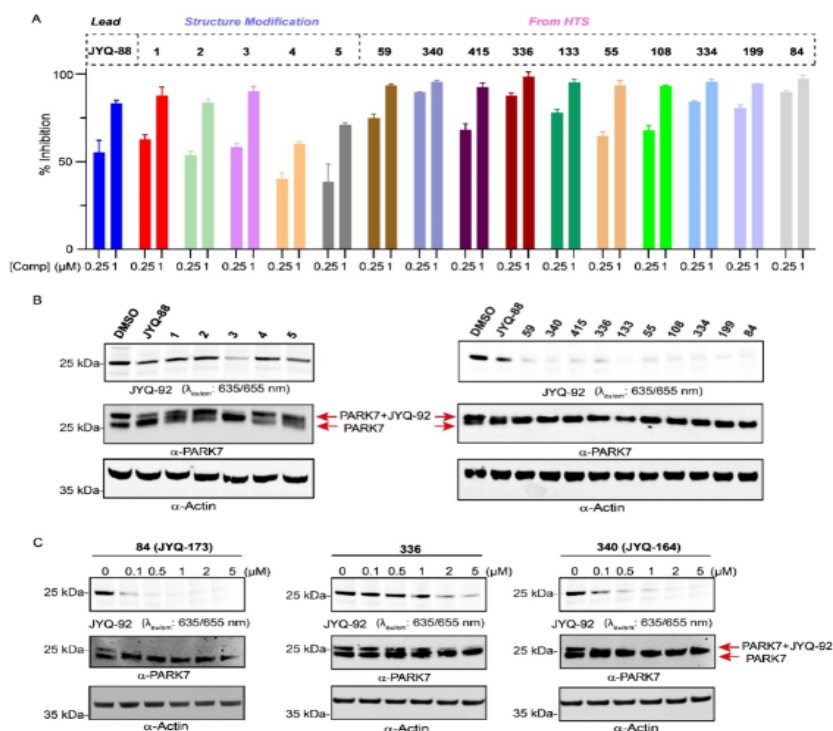


**Figure 2.** Assessment of potency and cell permeability of the selected compounds. (A) Inhibition of PARK7 at 0.25 and 1  $\mu$ M final concentration of 5 compounds designed from structural modification and top 10 compounds from HTS, determined using the PARK7 FP assay.<sup>15</sup> (B) Fluorescent probe labeling of PARK7 remaining activity after inhibitor treatment to investigate cellular engagement. HEK293T cells were treated with the indicated compounds for 24 h. After cell lysis and incubation with the fluorescent PARK7 probe JYQ-92 for 1 h, the samples were analyzed by SDS-PAGE, fluorescence scanning, and immunoblot against PARK7 and  $\beta$ -actin.  $\beta$ -Actin was used as a loading control. (C) Target engagement of compounds 84, 336, and 340 in HEK293T cells in a dose-response manner. HEK293T cells were incubated with the compounds at the indicated final concentrations for 24 h, prior to cell lysis and incubation with PARK7 probe JYQ-92. The samples were analyzed by SDS-PAGE, fluorescence scanning, and immunoblot against PARK7 and  $\beta$ -actin.  $\beta$ -Actin was used as a loading control.

Cyanamide-containing compounds reportedly effectively inhibit deubiquitinating enzymes (DUB). Therefore, using fluorescence-based DUB probe Rho-Ub-PAThe effects of compounds on cells were studied. To this end, the HEK293T cell lines used to evaluate DUB inhibitor. Among the compounds, only 4 kinds (108, 199, 334 and 415) show the DUB (mainly UCHL1), while other compounds (including the most potent 84, 336 and 340) does not show any DUB. Based on the potency and selectivity results, the compounds were selected 84, 336 and 340, and further evaluated their dose-dependent interactions with cells. PARK7 combination. HEK293T cells treated with these inhibitors 0.1–5  $\mu$ M. Dilution series treatment twenty four hours, then cells were lysed and probed. JYQ-92. Fluorescence scanning and Western blotting showed that the compound 84 and 340 from 0.1  $\mu$ M from the beginning. PARK7 combination, while compound 336. The effect is weak, from 1  $\mu$ M from PARK7 active combination (Fig. 2C). Therefore, it was decided to continue with the most potent, cell-permeable compounds 84 and 340, encoding JYQ-173 and JYQ-164, respectively, for further experiments (Figure 1G). As expected, based on the previous data for JYQ-88, intact protein mass spectrometry demonstrated that JYQ-164 and JYQ-173 covalently bind to PARK7 (Supporting Information Fig. S4). JYQ-88 and the previously reported indigo-based PARK7 inhibitors STK793590. Evaluation of the ability of JYQ-164 and JYQ-173 to inhibit PARK7 enzymatic activity. PARK7 active site dependent on the fluorescent substrate 6,8-difluoro-4-methylumbelliferyl Cys. JYQ-164 and JYQ-173 effectively inhibit PARK7 activity, with IC<sub>50</sub> values of 21 and 19 nM, respectively (Supporting Information Fig. S5A), which is 5-fold more potent than JYQ-88 (IC<sub>50</sub> 120 nM) and STK793590 (IC<sub>50</sub> 130 nM). These inhibitors also showed increased. With UCx. Compared with HL1, the selectivity for PARK7 differed by nearly 1000-fold (Supporting Information Fig. S5B and Table S1). After demonstrating the selectivity and potency of JYQ-164 and JYQ-173 for PARK7 in HEK293T cells, further experiments were performed in A549 cells, a lung adenocarcinoma model cell line. Hour. Finally, both compounds did not show any cytotoxicity in A549 cells up to 5  $\mu$ M but still exhibited complete inhibition of PARK7 binding to the JYQ-92 probe (Supporting Information Fig. S6).

#### **JYQ-164 and JYQ-173 are highly selective inhibitors of PARK7**

To investigate the selectivity of JYQ-164 and JYQ-173 in cells, a simplified cysteine activity-based protein assay (SLC-ABPP) was performed, which can be used to analyze and quantify reactive cysteines covalently bound to. A549 cells were treated with 0.5 or 5  $\mu$ M of each inhibitor together with DMSO control for 4 h, followed by cell lysis and incubation with a desthiobiotin iodoacetamide (DBIA) probe, which was used to differentiate and enrich for reactive cysteine sites that were not bound to JYQ-164 or JYQ-173. In addition, samples were digested with trypsin and endoGluC treated with tosylphenylalanylchloromethylketone (TPCK) to increase the coverage of protein sequences, especially the PARK7 peptide containing Cys106. Peptides generated by duplicate digestion of each sample were labeled with TMT16-plex to perform tandem mass tag (TMT)-based quantitative proteomics analysis. After TMT labeling, all samples were pooled and peptides conjugated to DBIA probes were enriched by streptavidin beads and analyzed by LC-MS/MS (Figure 3A). A total of

13,492 peptides containing cysteine sites were detected and listed according to the abundance ratio of all conditions (Supplementary Data S2). The abundance of each modified peptide was first calculated as the ratio between each replicate of different concentrations of JYQ-164 and JYQ-173 and the average abundance ratio of the DMSO samples of the same peptide (DMSO/inhibitor ratio). All cysteines were represented by the shortest peptide, and the average CR value of peptides with the same modified cysteine from the same protein under the same conditions was used. A total of 5,512 unique cysteine sites were quantified (Supplementary Data S3). Only cysteines with a competition ratio  $\geq 4$  (referred to as the CR threshold), corresponding to a  $\geq 75\%$  reduction in DBIA probe alkylation on either JYQ-164 or JYQ-173 cysteine, were considered targets (Fig. 3B–E). PARK7 Cys106 was identified as the only target site after treatment with 5  $\mu\text{M}$  JYQ-164, whereas no target sites showing a  $\geq 75\%$  reduction in DBIA probe alkylation were found after treatment with 0.5  $\mu\text{M}$  JYQ-164 (Fig. 3B,D). Furthermore, PARK7 Cys106 was identified as the only targeted cysteine with a  $\geq 75\%$  reduction in DBIA probe alkylation in JYQ-173-treated cells (0.5 and 5  $\mu\text{M}$ ) (Fig. 3C,E). Taken together, these data suggest that JYQ-164 and JYQ-173 are highly selective for PARK7 Cys106 and that JYQ-173 has higher potency than JYQ-164 for PARK7 in cells.

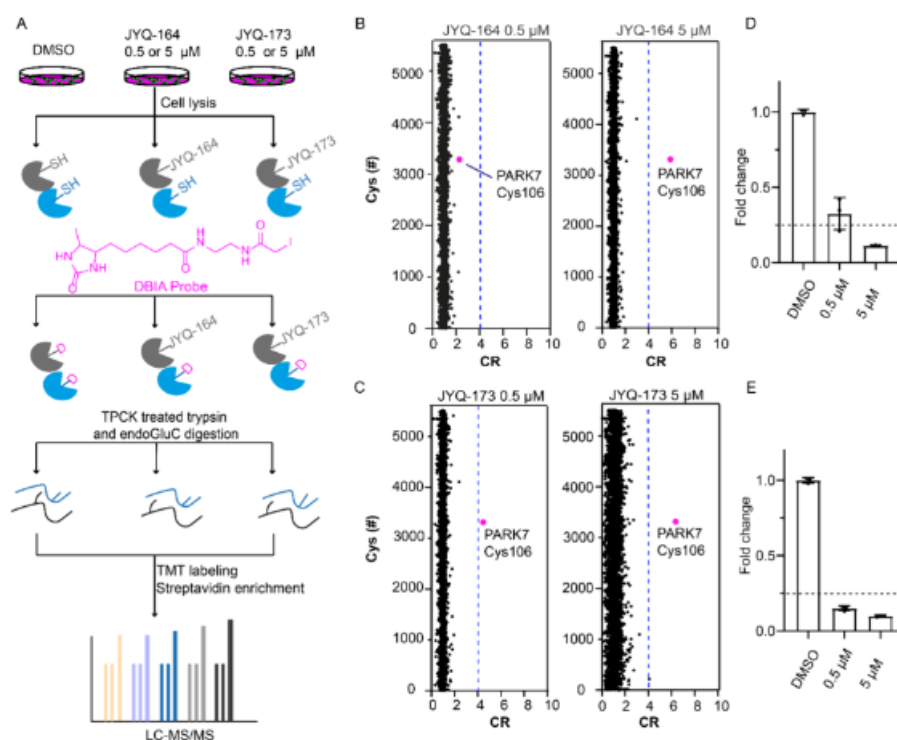


**Figure 3.** Investigation of the cellular selectivities of JYQ-164 and JYQ-173. (A) Schematic illustration of the workflow for the SLC-ABPP experiment. (B, C) SLC-ABPP profiling of PARK7 inhibitor JYQ-164 or JYQ-173 in A549 cells using two different concentrations (0.5 and 5  $\mu\text{M}$ ) quantified  $>5500$  cysteine sites. All experiments were performed in triplicates. Data are represented as means  $\pm$  s.d. Dotted lines represent a CR threshold of 4 (75% reduction in DBIA probe binding). (D, E) Fold changes of annotated peptide for PARK7 Cys106 residue in inhibitor-treated samples compared to a DMSO control are represented as a column graphic where the 0.25 fold change corresponding to 75% reduction in DBIA probe binding is highlighted with dotted lines.

### JYQ-164 and JYQ-173 become cell-permeable activity probes

Confirm that JYQ164 and JYQ-173 are highly efficient and selective for cellular PARK7, and are selected bycatchFluorescent dyes convert inhibitors into fluorescent, cell-permeable activity-based probes (ABPs).use SulfoCy5-Alkynes and

BodipyFL-Alkynes, using Catalyzes azide-alkyne cyclo-addition (or click) reactions. The triazole group already present in JYQ-173 was utilized. A new compound was synthesized by replacing the triazole part in JYQ-173 with an azide, which was converted to the corresponding triazole after a click reaction with a diyne to give probes JYQ-196 and JYQ-197 (Figure 4A, Scheme 2). Inhibitor JYQ-164 No suitable Therefore, the morpholine moiety was replaced with 4-azidoacetyl piperazine and reacted with alkynes to obtain probes JYQ-191 and JYQ-192 (Figure 4A, Scheme 2). These probes were evaluated for in vitro labeling and Visualization Capacity of PARK7 activity, use Recombinant human PARK7 protein (1  $\mu\text{M}$ ) was incubated with a series of probe concentrations at 37  $^{\circ}\text{C}$  and then subjected to SDS-PAGE analysis under non-denaturing conditions (without boiling and  $\beta$ -mercaptoethanol). Fluorescence scanning of the gel clearly showed that all four probes were able to label recombinant PARK7 in a dose-dependent manner. Labeling of PARK7 with the inhibitor JYQ-173-based probes JYQ-196 and JYQ-197 was more efficient than labeling with the inhibitor JYQ-164-based probes JYQ-191 and JYQ-192 (Figure 4B). The complete labeling of recombinant PARK7 by these probes could also be tracked using the band shifts caused by the Bodipy and SulfoCy5 probes. Coomassie staining showed that JYQ-196 and JYQ-197 completely labeled the recombinant PARK7 protein at 2 and 1  $\mu\text{M}$  concentrations, respectively. On the other hand, JYQ-191 achieved complete labeling at 5  $\mu\text{M}$  concentration, and JYQ-192 exist Complete labeling was achieved at 2  $\mu\text{M}$  concentration, which means that the JYQ-173-based probe had a higher labeling efficiency than the JYQ-164-based probe ( Figure 4B ).

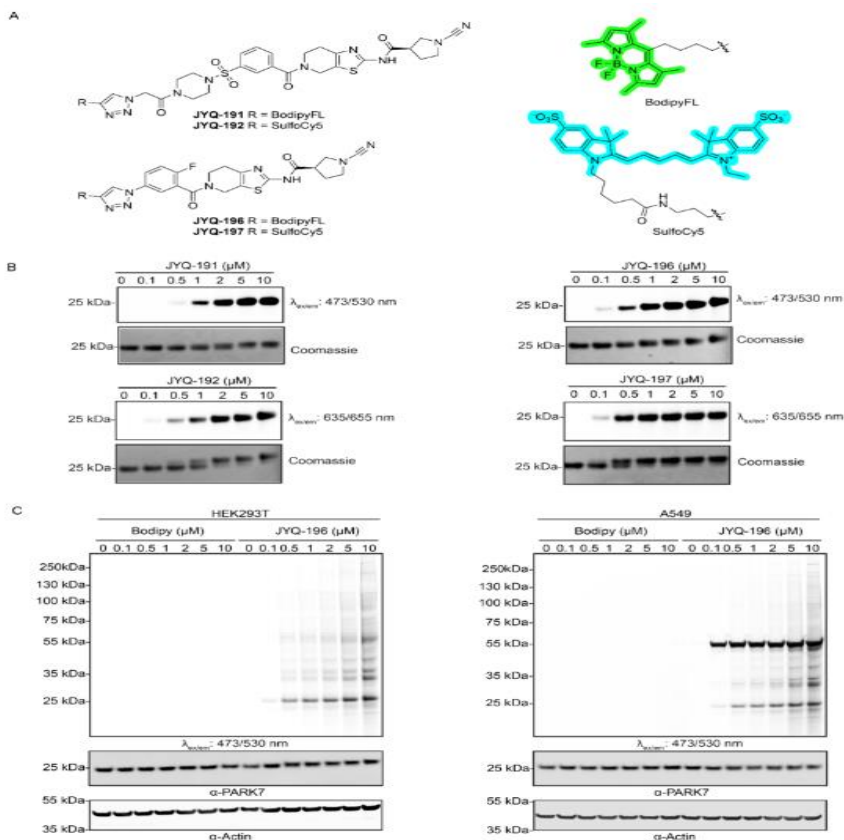


**Figure 4.** (A) Chemical structures of activity-based probes JYQ-191, JYQ-192, JYQ-196, and JYQ-197. (B) Labeling of purified recombinant human PARK7 with the four probes. Recombinant human PARK7 was incubated with indicated concentrations of the probes for 1 h followed by SDS-PAGE, fluorescence scanning, and coomassie staining. (C) Fluorescence labeling of PARK7 activity in HEK293T and A549 cells with JYQ-196. HEK293T and A549 cells were incubated with indicated final concentration of JYQ-196 for 4 h, followed by cell lysis, SDS-PAGE, fluorescence scanning, and immunoblotting against PARK7 and  $\beta$ -actin.  $\beta$ -Actin was used as a loading control.

To further investigate the ability of these probes to visualize PARK7 in cells, HEK293T and A549 cells were incubated with 5  $\mu$ M of these probes for 24 h, followed by cell lysis, SDS PAGE, fluorescence scanning, and immunostaining (Supporting Information Fig. S7). For two SulfoCy5 probes (JYQ-192 and JYQ-197, a clear band around 25 kD was observed) and the BodipyFL probe JYQ-196, corresponding to the expected mass of ABP-labeled PARK7. A band shift of PARK7 protein in samples treated with JYQ-192, JYQ-196, and JYQ-197 was also observed by immunoblotting of PARK7 in A549 cells. On the other hand, no band shift of PARK7 protein was observed in samples treated with the Bodipy probe JYQ-191, indicating that the labeling efficiency of cellular PARK7 by this probe was low. Therefore, JYQ-192, JYQ-196, and JYQ-197 were further investigated. To characterize their cell permeability, A549 cells were incubated with these probes at a final concentration of 5  $\mu$ M for the indicated time points, followed by confocal microscopy and cell lysis, SDS-PAGE, fluorescence scanning, and immunostaining. All three probes had entered the cells after 1 incubation (Supporting Information Fig. S8A). However, only the Bodipy probe JYQ-196 showed complete labeling of cellular PARK7 after 4 incubations, while the SulfoCy5 probes JYQ-192 and JYQ-197 labeled a small fraction of cellular PARK7 even after 24 incubations (Supporting Information Fig. S8B), indicating poor targeting of JYQ-192 and JYQ-197 in intact cells. In addition to PARK7, additional bands were observed in the fluorescence scanning of HEK293T and A549 cells, and very strong band labeling was observed between 55 and 75 kDa in A549 cells at a final concentration of 5  $\mu$ M for all probes.

Although the probe JYQ-196 was superior to the SulfoCy5 probes JYQ-192 and JYQ-197 in terms of cell PARK7 labeling efficiency, the probe still lacks specificity. PARK7 forms dimers, trimers, and even high molecular weight complexes under non-reducing conditions. Therefore, to examine whether these additional bands are markers of different forms of PARK7, PARK7 was depleted in HEK293T and A549 cells by siRNA transfection, and control cells were subsequently incubated with JYQ-196 at a final concentration of 5  $\mu$ M. The disappearance of a clear band corresponding to PARK7 was observed in the PARK7-depleted samples, while other bands did not show any changes compared with the control samples (Supporting Information Figure S9), indicating that JYQ-196 nonspecifically labeled other proteins. To further investigate whether lower concentrations of JYQ-196 could reduce nonspecific labeling, HEK293T and A549 cells were incubated in increasing concentrations (0–10  $\mu$ M) of JYQ-196 for 4 h, followed by cell lysis, SDS-PAGE, fluorescence scanning, and immunostaining (Figure 4C). This showed that lower concentrations of JYQ-196 could still effectively label PARK7 while exhibiting less nonspecific labeling.

#### **PROTAC derived from JYQ-173 provides functional cellular PARK7 degrader**

After successfully converting the inhibitors into cell-permeable ABPs, the option of generating proteolysis-targeting chimeras (PROTACs) was investigated. PROTACs are heterobifunctional molecules that bind to an E3 ligase and a protein of interest (POI) to form a ternary complex, thereby targeting the proteasome to degrade the POI.

Therefore, a group of PROTACs were designed and synthesized: JYQ-187 and JYQ-188 (based on the inhibitor JYQ-164) and JYQ-194 and JYQ-195 (based on the inhibitor JYQ-173), using a similar approach to the ABPs described above. Use The cereblon ligand pomalidomide was linked to two PEG linkers of different lengths (Figure 5A, Scheme 3, Supporting Information Figure S10A). Their ability to induce PARK7 degradation in A549 cells was evaluated by treating them with increasing concentrations of PROTACs (from 0.1 to 5  $\mu\text{M}$ ) for 8 h. Among them, JYQ194 emerged as the most potent PARK7 degrader, inducing PARK7 degradation starting from 0.1  $\mu\text{M}$  and reaching approximately 80% of Dmax at a concentration of 5  $\mu\text{M}$  (Figure 5B, C). JYQ-195The efficiency of JYQ-194 was low because it started to degrade PARK7 from 2  $\mu\text{M}$ . Degradation of PARK7 was observed with JYQ-187 and JYQ-188, both of which are based on JYQ-164 (Supporting Information Figure S10B). Therefore, JYQ-194 was selected for further evaluation.

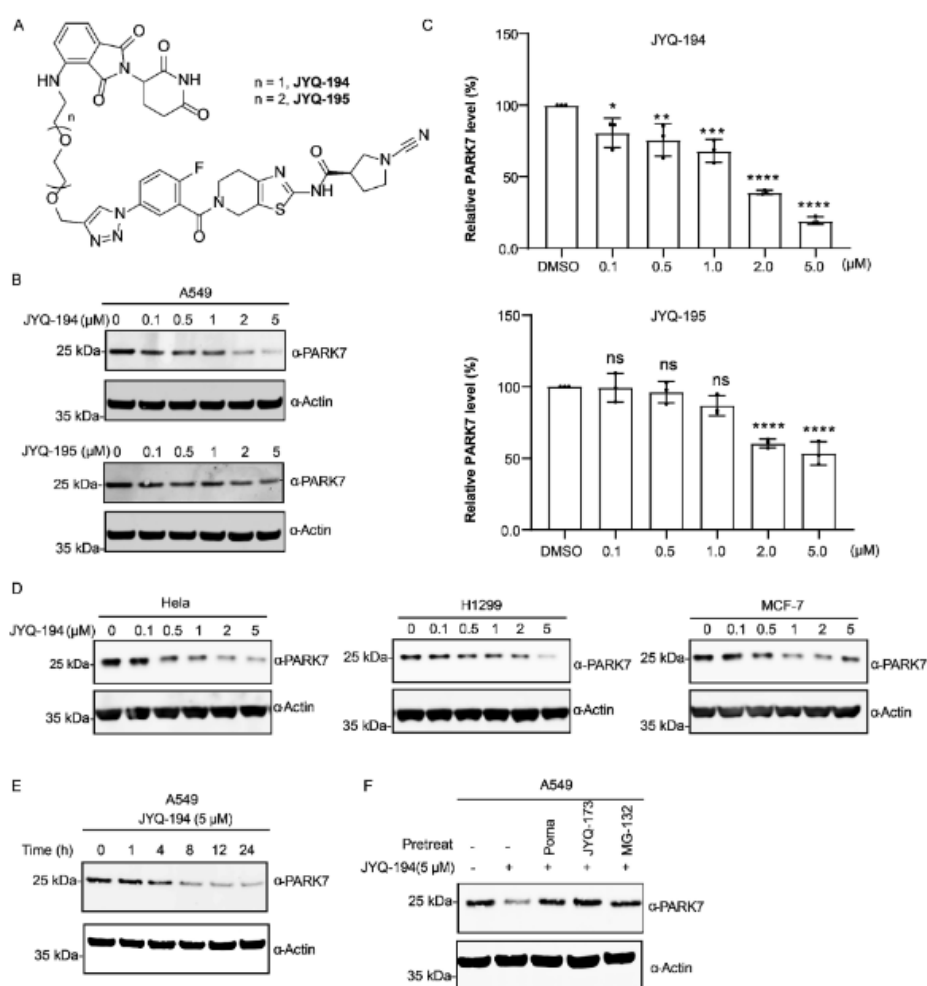


**Figure 5.** (A) Structures of PROTACs JYQ-194, JYQ-195. (B) PARK7 degradation efficacy with PROTACs JYQ-194, JYQ-195. A549 cells were incubated with the indicated concentration of PROTACs JYQ-194 and JYQ-195 for 8 h, followed by cell lysis, SDS-PAGE, and immunoblot analysis. (C) Quantification of Western blot of JYQ-194, JYQ-195 in panel B. Total PARK7 protein levels at each concentration of JYQ-194 were normalized to a DMSO control. Quantified data represent mean  $\pm$  SD for three independent biological replicates. All significance was calculated using standard Student's *t* test: \**p* < 0.05, \*\**p* < 0.01, \*\*\**p* < 0.001. (D) JYQ-194 induces PARK7 degradation in multiple tumor cell lines. Cells were treated with indicated concentrations of JYQ-194 for 8 h, followed by cell lysis and immunoblot analysis. (E) Time-course experiment for JYQ-194 (5  $\mu\text{M}$ ). A549 cells were treated with JYQ-194 (5  $\mu\text{M}$ ) for the indicated time, followed by cell lysis, running SDS-PAGE gel, and immunoblot analysis. (F) PARK7 degradation relies on ternary complex formation and proteasomal degradation. A549 cells were pretreated with 5  $\mu\text{M}$  CRBN binder pomalidomide (POMA), 5  $\mu\text{M}$  PARK7 inhibitor JYQ-173, or proteasome inhibitor 10  $\mu\text{M}$  MG-132 for 4 h, followed by treatment with JYQ-194 (5  $\mu\text{M}$ ) for additional 8 h. Following cell lysis, the samples were run in SDS-PAGE gel, and immunoblot analysis was performed. All immunoblots performed in this figure were against PARK7 and  $\beta$ -actin.  $\beta$ -Actin was used as a loading control.

Next, the efficiency of JYQ-194-induced PARK7 degradation in multiple tumor cell lines, including HeLa, H1299, and MCF7, was determined. PARK7 degradation was observed in all of these cells in a dose-dependent manner (Figure 5D). To explore the kinetics of PARK7 degradation in JYQ-194-induced cells, experiments were performed in A549 cells using a fixed concentration of 5  $\mu$ M JYQ-194, which has been shown to induce maximal degradation in all cell lines tested. Degradation of PARK7 was observed starting at 4 hours, and maximal degradation of PARK7 was not observed until 24 hours (Figure 5E). To test the functionality of each component of the JYQ-194 PROTAC and investigate whether PARK7 degradation is indeed dependent on the ubiquitin proteasome system, A549 cells were pre-treated with the CRBN binder pomalidomide, the PARK7 inhibitor JYQ-173, or the proteasome inhibitor MG132 for 4 hours. Then JYQ-194 incubation. Other additional Each inhibitor targeting a functional PROTAC and a single component of the proteasome abolished PARK7 degradation ( Figure 5F ), indicating that degradation of the ubiquitin/proteasome system by JYQ-194 is PARK-dependent. Selective induction of PARK7 degradation. To explore the degradation selectivity of PROTAC JYQ-194 for PARK7, TMT-based quantitative total proteome analysis was performed by incubating A549 cells with 5  $\mu$ M JYQ194 and 5  $\mu$ M JYQ-173 and DMSO as a control for 8 h (Figure 6A). More than 6,000 proteins were identified in the samples (Supplementary Data S4). JYQ-194 induced the degradation of PARK7. JYQ-173 did not change PARK7 protein levels (Figure 6B). Proteomic data also showed that TM7SF3 and DOP1B were reduced by PROTAC JYQ-194, while these proteins were also downregulated by the inhibitor JYQ-173 (Figure 6B), indicating that the downregulation of these two proteins is associated with the Cys106-dependent function of PARK7. In addition, unlike the inhibitor JYQ-173, PROTAC JYQ-194 partially reduced HINT2 (histidine trinucleotide binding protein 2), which means that HINT2 may be an off-target of PROTAC JYQ-194 or may be regulated by the PARK7 backbone function. PARK7 remains the main target of JYQ-194. Collectively, these findings suggest that JYQ-194 is a selective degrader of PARK7.

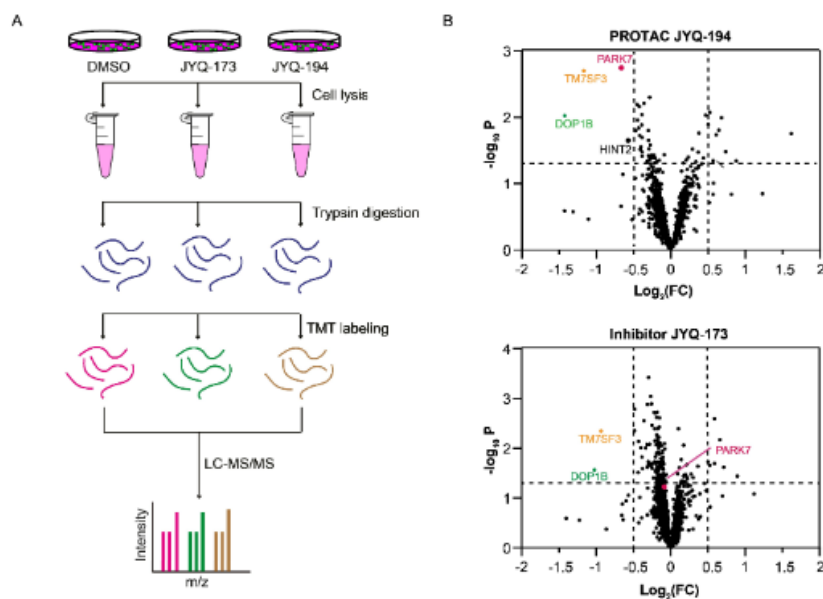


**Figure 6.** (A) Schematic illustration of the workflow of TMT-based total proteomics experiments. A549 cells were incubated with DMSO, JYQ-173, or JYQ-164 for 8 h. Upon cell lysis and trypsin digestion, the peptides were labeled with TMTpro label reagents, and samples were pooled for LC-MS/MS analysis. (B) Proteomics analysis of proteins differentially expressed in PROTAC JYQ-194 and inhibitor JYQ-173-treated A549 cells compared to DMSO-treated A549 cells. Volcano plots of the  $-\log_{10}(p\text{-value})$  versus the  $\log_2$  fold change (FC) for JYQ-194 versus DMSO (top panel) and JYQ-173 versus DMSO (bottom panel). All the samples were prepared as  $n = 3$  biological replicates. Proteins with  $-\log_{10}(p\text{-value}) > 1.3$  and  $\log_2 \text{FC} < -0.5$  or  $\log_2 \text{FC} > 0.5$  were considered to be significantly changed in abundance.  $p$ -Values were calculated using standard Student's  $t$ -test.

### in conclusion

In addition to being potential therapeutic agents, small molecule inhibitors are also important tools for studying the biological functions of specific proteins, especially enzymes, by binding to them and affecting their cellular functions through catalytic or allosteric mechanisms. These inhibitors also provide opportunities for the design and expansion of chemical tools. For example, activity-based probes (ABPs) and protein degraders (PROTACs) have laid the foundation. Combining these chemical tools derived from similar structures can help study different perspectives of target proteins in vitro, in living cells, and even in complex animal models. By using recently developed high-throughput screening compatible FP experiment, this article reports the development of JYQ-164 and JYQ-173, potent and selective inhibitors of PARK7, an attractive therapeutic target. Both compounds effectively inhibited PARK7 enzyme activity with IC<sub>50</sub> values of 19 and 21 nM, respectively, which was 5-fold higher than the previously reported inhibitor JYQ-88. Optimization of the 2-azidoacetyl moiety in JYQ-88 was aimed at occupying the protein pocket surrounding this moiety, which is largely unoccupied. In vitro FP experiments performed on 15 purified compounds showed that the introduction of aromatic substituents favored the inhibitory potency, whereas aromatic hydrophilic moieties did not improve (compounds 1 and 2) or even reduced (compounds 4 and 5) the potency. Interestingly, all compounds showing improved inhibition contained an aromatic moiety substituted at the meta position. Notably, direct targeting of the inhibitors JYQ-164 and JYQ-173 in living cells was shown in a cell-based competition assay. Intracellular SLC-ABP analysis demonstrated that these compounds specifically target the highly conserved Cys106 of PARK7, a residue that is essential for the biological function of PARK7 and for sensitivity to oxidative stress. With these potent and selective inhibitors, four

activity-based probes were designed and synthesized: JYQ-191, JYQ-192, JYQ-196, and JYQ-197, by installing Bodipy or SulfoCy5 dyes on them. Probe JYQ-196, by Continue Bodipy dye, derived from JYQ-173, outperforms other probes by efficiently labeling PARK7 activity in living cells. **JYQ-196** It also exhibited nonspecific labeling of other proteins in labeling experiments, whereas the original compound JYQ-173 showed high selectivity for PARK7 in SLC-ABPP experiments. The probe proposed here has a great advantage because cellular PARK7 can be labeled with high efficiency in one step without the need for an intermediate click chemistry reaction, thereby eliminating all the disadvantages associated with two-step labeling. Therefore, the probe may serve as a diagnostic tool in further efforts, as PARK7 is a potential biomarker for various cancers and Parkinson's disease. In addition, further development of a selective PARK7 degrader, JYQ-194, induces PARK7 degradation in different tumor cell lines. The covalent, irreversible nature of JYQ-194 may limit its potency, as it cannot be recovered after PARK7 degradation, which may reduce its efficacy in the in vivo setting. Despite its limitations, JYQ-194 PROTAC provides new opportunities for targeting PARK7 in cancer therapy, as PARK7 is overexpressed in various types of cancer.

In summary, the chemistry of PARK7 has been greatly expanded by developing two cell-permeable, potent, and specific PARK7 inhibitors, two activity-based probes for monitoring or visualizing PARK7 activity in cells, and a selective degrader for inducing PARK7 degradation. The articles supply OverPotent and selective inhibitors, ABPs, and PROTACs, these chemical tools will help elucidate the biological functions of PARK7 in health and disease and explore possible future therapeutic drugs for PARK7.

Source: <https://doi.org/10.1021/acs.jmedchem.3c02410>

### Part 3

1. CyberSAR combines drug design ideas and mines the active structures reported in literature and patents. Through CyberSAR, researchers can quickly and easily obtain the target structures of interest to them, so as to explore new ideas. The following is an example of PARK7 Parkinson disease protein 7 (Homo sapiens):

Home > Target Overview > Target Detail

**PARK7 : Parkinson disease protein 7 (Homo sapiens)**

Structure Info

Indication

ChemSpace

Assay Data

Bioassay

SAR Doc

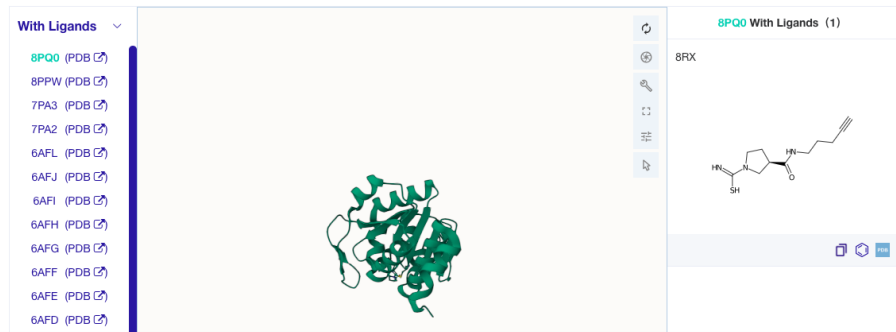
Target Landscape

**Name And Taxonomy**

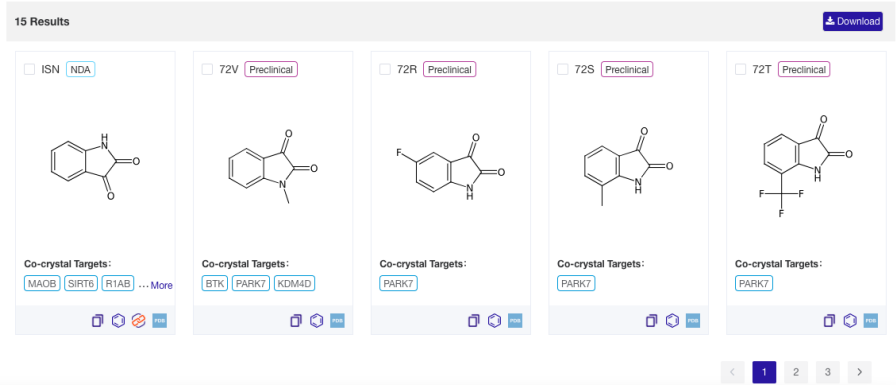
Name	Parkinson disease protein 7
Synonyms	帕金森氏病蛋白7   Parkinsonism-associated deglycase   Protein/nucleic acid deglycase DJ-1   Protein DJ-1   Maillard deglycase   DJ-1   Oncogene DJ1
Organism	Homo sapiens
Class	Enzyme   Hydrolase
Type	SINGLE PROTEIN
Ext. Links	<a href="#">GenCards</a>   <a href="#">OpenTarget</a>   <a href="#">UniProt</a>   <a href="#">PDB</a>   <a href="#">AlphaFold</a>
Physiological	Multifunctional protein with controversial molecular function which plays an important role in cell protection against oxidative stress and cell death...
Function	<a href="#">More</a>

Components

3D Structure



Ligands



2. In the target interface, select the "Chemical Space" option tab and cascade the "Cluster Structure View" tab to display the literature and patents collected by the CyberSAR platform with relevant **PARK7**. The molecules tested for activity in related experiments are displayed in the form of "core structure clusters". The green highlighted ones are the active molecular structures with  $IC_{50} < 1000$  nM in in vitro enzyme and cell activity test experiments reported in the literature, as well as the specific experiments, experimental results and experimental sources.

Home > Target Overview > Target Detail

**PARK7 : Parkinson disease protein 7 (Homo sapiens)**

Structure Info  
 Indication  
**ChemSpace**  
 Assay Data  
 Bioassay  
 SAR Doc

Target Landscape

Real Structure Cluster Structure (32) Clustering Threshold Loose Strict

Tips: 1- The chemical space includes molecules labeled manually and those identified through experimental data mining; 2- Manual labels are sourced from the Pharmacodia global drug database and other manually confirmed sources; Active molecules are those with activity indicators  $\leq 1000$  nM; 3- The R&D status reflects the highest development status of the molecules contained in the cluster.

Cluster ID	Chemical Structure	Clustering Threshold	Clustering Status	Clustering Count	Active Count	Clinical Count
CC331359		Loose	Active	2219	0	21 (Approved)
CC332041		Loose	Active	497	2	8 (Approved)
CC334848		Loose	Active	447	6	1 (Approved)

Pharmacodia Global Assay Data | CC332041 2 Results

**CYBER** Pharmacodia AI

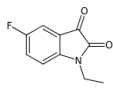
Home > Target Overview > T

**PARK7 : Parkinson**

Structure Info  
Indication  
**ChemSpace**  
Assay Data  
Bioassay  
SAR Doc

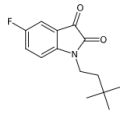
Target Landscape

C986587 Preclinical



IC50 = 118 nM  
Inhibition of pET3a-His-tagged DJ1 (unknown origin) expressed in Escherichia coli BL21 assessed as decrease in esterase activity using 10.1039/D1MD00062D

C1001129 Preclinical



IC50 = 851 nM  
Inhibition of pET3a-His-tagged DJ1 (unknown origin) expressed in Escherichia coli BL21 assessed as decrease in esterase activity using 10.1039/D1MD00062D

< 1 >

3. In the target interface, select the "Chemical Space" option tab and cascade the "Original Structure View" tab to display the literature collected by the CyberSAR platform with relevant PAK7. The molecules tested for activity in related experiments are displayed in the form of a "timeline of research and development stages". The "data mining" highlighted in green font is the potential hit.

Home CyberSAR Known SAR map CyberX-Discovery AI-driven drug discovery toolkit CyberX-Virtual Library Real-based virtual compound libraries Customized Services 中 | En

Home > Target Overview > Target Detail

**PARK7 : Parkinson disease protein 7 (Homo sapiens)**

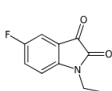
Structure Info  
Indication  
**ChemSpace**  
Assay Data  
Bioassay  
SAR Doc

Target Landscape

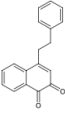
Real Structure (481) Cluster Structure (32) Data Range Manual Label Data Mining

Tips: 1- The chemical space includes molecules labeled manually and those identified through experimental data mining; 2- The R&D status reflects the highest development status of the molecules.

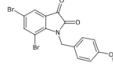
Preclinical (481)  
Manual Label 466  
Data Mining 15



C986587  
Assay Data



C1005652  
Assay Data



C980542  
Assay Data



C997065  
Assay Data

To Explore Cyber-AIDD further Login on your computer using the below Link

<https://cyber.pharmacodia.com/#/homePage>

If you need further assistance, contact us,

**For a free trial, Contact us on**

**Anil Ranadev**

+91 9742627845

anil\_ranadev@saspinjara.com

**Aravind P**

+91 9619076286

aravind.p@saspinjara.com

**Sachin Marihal**

+91 9538033363

sachin.marihal@saspinjara.com

**Chetan S**

+91 7022031061

chetans@saspinjara.com

